FINAL TECHNICAL REPORT

USGS AWARD 07HQGR0070

3D Modeling of Spontaneous Earthquake Sequences with Application to Parkfield

Principal Investigator: Nadia Lapusta
California Institute of Technology
1200 E. California Blvd., M/C 104-44
Pasadena, CA 91125
(626) 395-2277, Fax: (626) 568-2719
lapusta@caltech.edu

Abstract

Small repeating earthquakes have been found in California, Japan, and Taiwan and their observations have been used to study various aspects of earthquake physics and mechanics. In part, they are used for inferring the creeping rates of the surrounding fault segments. Because of their short recurrence times and known locations, small repeating earthquakes present a rare predictable opportunity for detailed observation and study, and that has been exploited in the San Andreas Fault Observatory at Depth (SAFOD) drilling project. It is important to establish realistic models for their occurrence, to provide a framework for proper interpretation of SAFOD data and other studies. Before SAFOD, the most intriguing observation about repeating earthquakes had been the scaling of their repeat time T and seismic moment M_0 as $T \sim M_0^{0.17}$. The scaling is abnormal compared to other earthquakes that have $T \sim M_0^{1/3}$, the typical scaling that results from a simple conceptual model. Several explanations for the discrepancy in scaling have been proposed, each of them containing assumptions the validity of which is either unclear or disputed.

Our studies supported by USGS have shown that a model based on laboratory-derived rate and state friction laws reproduces the observed abnormal scaling. The resulting repeating earthquakes have typical stress drops. In our 3D model, a small patch with rate-weakening friction is surrounded by a much larger region with rate-strengthening friction. For a set of realistic parameters, we can reproduce the observed scaling simply by varying the size of the rate-weakening patch. Our simulations use 3D numerical methodology that fully resolves all aspects of seismic and aseismic behavior of the fault, including slow tectonic loading, inertial effects during seismic slip, and accelerating and decelerating aseismic slip. We have further developed the numerical methodology as part of this project. In simulations, much of slip in the patch is accumulated aseismically, even though the patch also produces seismic events. From a more general point of view, the studies have advanced our understanding of the partition of slip into seismic and aseismic parts and their interaction. These results and the developed methodology can be applied to other cases of interaction between seismic and aseismic slip, such as aseismic slip transients and associated low-frequency seismic tremor.

Publications supported by this project:

Chen, T. and N. Lapusta, Scaling of small repeating earthquakes explained by interaction of seismic and aseismic slip in a rate and state fault model, submitted to *J. Geophys. Res.*, 2008.

Lapusta, N, and Y. Liu, 3D boundary-integral modeling of spontaneous earthquake sequences and aseismic slip, submitted to *J. Geophys. Res.*, 2008.

Small repeating earthquakes, their abnormal scaling, relevance to SAFOD project

Small repeating earthquakes have been found in California, Japan, and Taiwan and their observations have been used to study various aspects of earthquake physics and mechanics (e.g., Ellsworth and Dietz, 1990; Vidale et al., 1994; Marone et al., 1995; Nadeau and Johnson, 1998; Beeler et al., 2001; Sammis and Rice, 2001; Igarashi et al., 2003; Chen and Rau, 2003; Imanishi et al., 2004; Nadeau et al., 2004). Because of their short recurrence times and known location, small repeating earthquakes present a rare predictable opportunity for detailed observation and study, and that has been exploited in San Andreas Fault Observatory at Depth (SAFOD) drilling project (e.g., Imanishi et al., 2004).

Before the detailed SAFOD data, the most intriguing observation about repeating earthquakes had been the scaling of their repeat time T with their seismic moment M_0 as $T \sim M_0^{0.17}$ (Nadeau and Johnson, 1998). This scaling is abnormal compared to other earthquakes that have $T \sim M_0^{1/3}$, the typical scaling that results from a simple conceptual model in which earthquakes are treated as circular ruptures with stress drop independent of the seismic moment and slip that is proportional to the repeat time. Several explanations for the discrepancy in scaling have been proposed, including dependence of stress drop on seismic moment, with much higher stress drops for small events (Nadeau and Johnson, 1998), and occurrence of repeating earthquakes at a border between large locked and creeping patches (Sammis and Rice, 2001). However, there is no evidence for a large locked asperity and recent studies based on SAFOD data indicate that stress drops for repeating earthquakes fall into the typical range. Beeler et al. (2001) considered the model of a fixed-area patch governed by a conceptual law that incorporated strain-hardening. They showed that aseismic slip on the patch can explain the observed scaling relation. However, the work pointed out that there was no experimental evidence for the strain-hardening law used in the model.

SAFOD is a unique facility for studying the earthquake source. Since its targets are small repeating earthquakes, it is very important to establish realistic models for their occurrence, to provide a framework for proper interpretation of SAFOD data. SAFOD location ensures that seismic, pore-pressure, tilt, and temperature data will be captured in unprecedented proximity for several repeating earthquakes and processes before and after them. Proximity is an important advantage of SAFOD, as it not only allows to capture variations that may not be observable at a greater distance but also significantly improves the ability to separate the signal into path effects and source contributions. Following the completion of the Phase 3 core drilling, the multi-parameter long-term monitoring system will be installed within the fault core and damage zone of the San Andreas Fault at the location of a repeating microearthquake (M 1.8–2.0). This provides a unique opportunity for comparison with detailed physics-based simulations that have been developed in this project.

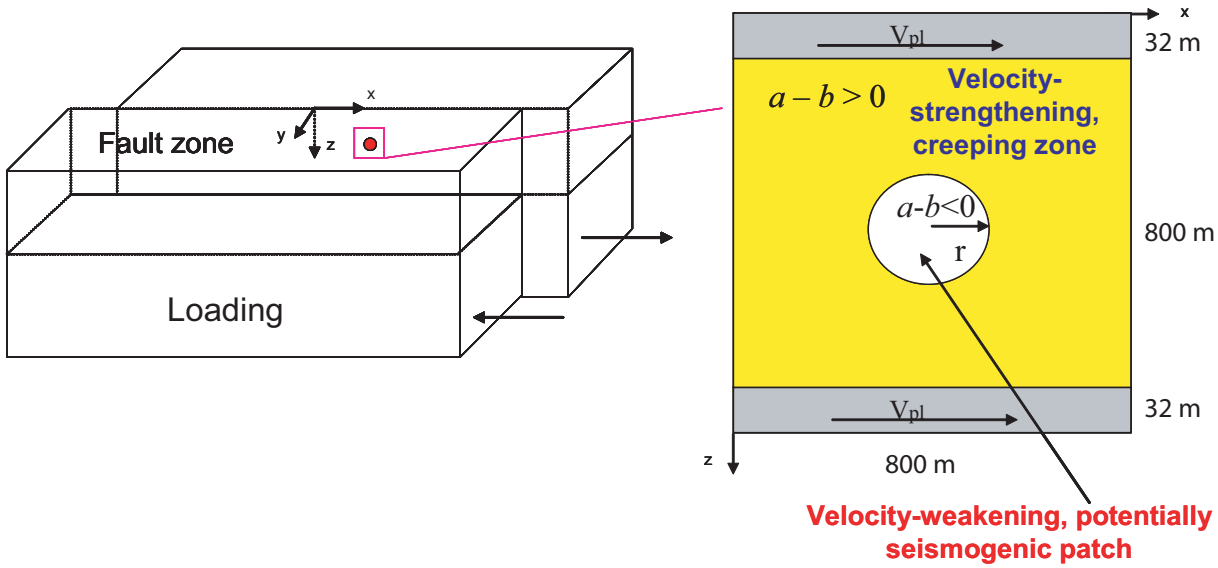

Figure 1. The schematics of our model for small repeating earthquakes. Left panel: a vertical strike-slip fault governed by rate and state friction is embedded into an elastic medium. Right panel: We consider a creeping segment of the fault, governed by velocity-strengthening (also called rate-strengthening) friction, which contains a small potentially seismogenic patch, governed by velocity-weakening friction. Outside of the simulated creeping zone, we impose steady sliding with the loading rate V_{pl}, to represent the effect of the surrounding steadily creeping segment. We choose the size of the creeping (yellow) zone large enough so that the behavior of the velocity-weakening patch does not depend on the size of the creeping zone.

Model of small repeating earthquakes based on rate and state friction

Our model for the occurrence of small repeating earthquakes is shown in Figure 1. We consider a creeping segment of a planar strike-slip fault imbedded into an elastic medium. Zooming in on the location of a repeating earthquake, we construct a model consisting of a small circular seismogenic patch surrounded by a much larger creeping fault zone. Outside of the creeping zone, we impose sliding with the tectonic loading rate V_{pl}, to represent the effect of the surrounding steadily creeping segment.

The seismogenic and creeping parts of the fault are modeled by laboratory-derived rate and state friction laws which model variations of frictional shear strength τ_f due to its dependence on the effective normal stress $\bar{\sigma}$, slip rate V (which we also call slip velocity), and evolving properties (state) of the contact population represented by the state variable θ (e.g., Dieterich, 1979, 1981; Ruina, 1983). The state of the contact population depends on slip rate V but, for slip-rate changes, evolves with slip δ and hence reflects the intrinsically mixed rate-dependent and slip-dependent aspects of friction. The rate and state features can be thought of as, usually, small variations (of the order of 1-10%) from the baseline frictional strength given by $\bar{\sigma} f_o$. Despite being small, these variations are fundamentally important for physically and mathematically meaningful stability properties of frictional sliding, as can be shown through

linearized analysis of elastodynamic stability of frictional sliding to a Fourier mode perturbation for a general class of rate and state friction laws (e.g., Rice, Lapusta, and Ranjith, 2001). In our studies of small repeating earthquakes, we have used the standard Dieterich-Ruina rate and state friction formulation:

$$\tau_f = \bar{\sigma} f = (\sigma - p)[f_o + a\ln(V/V_o) + b\ln(V_o\theta/L)], \quad \frac{\partial\theta}{\partial t} = 1 - \frac{V\theta}{L}, \qquad (1)$$

where σ is the normal traction, p is the pore pressure (which could be evolving but is fixed in the current version of the model), f_o, V_o, a, b, and L are parameters of the standard rate and state friction, with L being the characteristic slip for state variable evolution.

Based on the encouraging results of this project, we plan, in the future, to explore the model response with other rate and state friction formulations, as well as with rate and state friction combined with dynamic weakening effects, such as flash heating.

Numerical simulations that resolve both seismic and aseismic slip

To solve for spontaneous long-term slip history in this model, we have further developed (Lapusta and Liu, 2009) the 3D simulation methodology which is the extension of the 2D methodology of Lapusta et al. (2000). The methodology incorporates laboratory-derived rate and state friction laws, slow tectonic-type loading, and all dynamic effects of self-driven dynamic rupture**.** Such modeling is very challenging, especially in 3D, because of the variety of temporal scales involved. Slow loading requires years in simulated time. At the same time, rapid changes in stress and slip rate at the propagating dynamic rupture tips occur over times of order a small fraction of a second. The algorithm combines these scales and allows to treat accurately long deformation histories and to calculate, for each earthquake episode, initially quasi-static accelerating slip (nucleation process), the following dynamic rupture break-out and propagation, postseismic response, and ongoing slippage throughout the loading period in creeping fault region.

Our 3D methodology fully resolves all stages of earthquake cycle and transitions between them, while approaches used by other researchers to model long-term slip histories have to compromise on some of these stages. They either treat the dynamic rupture propagation in a simplified way (e.g., 3D studies of Rice and Ben-Zion, 1996), or neglect all aseismic slippage (e.g., Cochard and Madariaga, 1996), or make the tectonic loading orders of magnitude faster (Shaw and Rice, 2000), or switch abruptly between quasi-static and dynamic methods, potentially disrupting nucleation processes (e.g., Shibazaki and Matsu'ura, 1992). Our solution methodology is based on a boundary integral spectral formulation and incorporates two main ideas: variable time stepping and justifiable truncation of dynamic response. The boundary-integral relations we use (Perrin et al., 1995; Geubelle and Rice, 1995) incorporate all elastodynamic interactions and involve the dependence of shear stress on current slip as well as relevant slip velocity history. There are no kinematic assumptions in this model other than the steady slip of the fault far from the location of the repeating earthquake.

To extend the methodology to 3D, we have proposed a numerical resolution criterion that combines findings for long-term histories and dynamic rupture, developed a new frequency-dependent truncation procedure, determined the values of numerical parameters that lead to

results independent of numerical procedures in three dimensions, and developed a parallel implementation of the 3-D code (Lapusta and Liu, 2008). Substantial part of this development has occurred as a part of this project.

Model response and slip partitioning into seismic and aseismic parts

In numerical simulations, our model produces repeating earthquakes embedded within a creeping region. As predicted by stability studies of sliding on rate and state faults (e.g., Rice, Lapusta, Ranjith, 2001), the rate-strengthening (also called velocity-strengthening) part of the fault accumulates slip through stable sliding, with slip velocities approaching the imposed loading rate farther from the patch. The rate-weakening patch, if small enough, smaller than theoretical estimates of nucleation sizes, also accumulates slip through stable, but slightly accelerating and decelerating, sliding. Larger rate-weakening patches produce repeating earthquakes.

A simulation example with repeating earthquakes is shown in Figure 2. Repeat time T is straightforward to get from the simulations. For each event, we compute the seismic moment M_0 as the moment released when the maximum slip velocity on the fault is larger than 1 cm/s. Figure 2 clearly shows that the seismic moment is a small fraction of the total moment released on the patch. Much of slip on the patch is released through pre- and post-seismic creep (or aseismic slip).

Figure 3 demonstrates one earthquake cycle using the first event as an example. At the beginning of the simulation, the whole velocity-weakening (and potentially seismogenic) patch is locked. As the imposed creep far from the patch continues, the locked area shrinks due to penetration of creep from the velocity-strengthening zone surrounding the patch. Eventually, fast (seismic) slip occurs. Postseismic slip continues on the patch for a while. Finally, the patch becomes locked again (not shown), and the earthquake cycle repeats.

The ability of the model to match the observed abnormal scaling of repeating earthquakes with typical stress drops

To obtain repeating earthquakes of different sizes, we change the size of the velocity-weakening patch, keeping all other parameters the same. The resulting scaling relationship between the repeat time T and the seismic moment M_0 reproduces the observed abnormal scaling as shown in Figure 4a. Green dots show our results for the applied loading rate V_{pl} of 23 mm/yr, used by Nadeau and Johnson (1998).

The best fit of the simulated results indicates a scaling relationship $T \sim M_0^{0.21}$, very similar to the observed $T \sim M_0^{0.17}$. However, this value of loading rate results in lower repeat times than the observed ones (the line fit to observations is given by the top line). If we use the applied loading rate of 4.5 mm/yr, which is within the range of 4 to 35 mm/yr suggested by Harris and Segall (1987) for the portion of the San Andreas fault with repeating earthquakes, then our model can reproduce both the scaling and the absolute values of the observed repeat times, as shown by blue triangles.

It is important to point out that the extent of seismic slip, indicated by the red color in Figure 3, is actually a small fraction of the assumed velocity-weakening patch. This is because

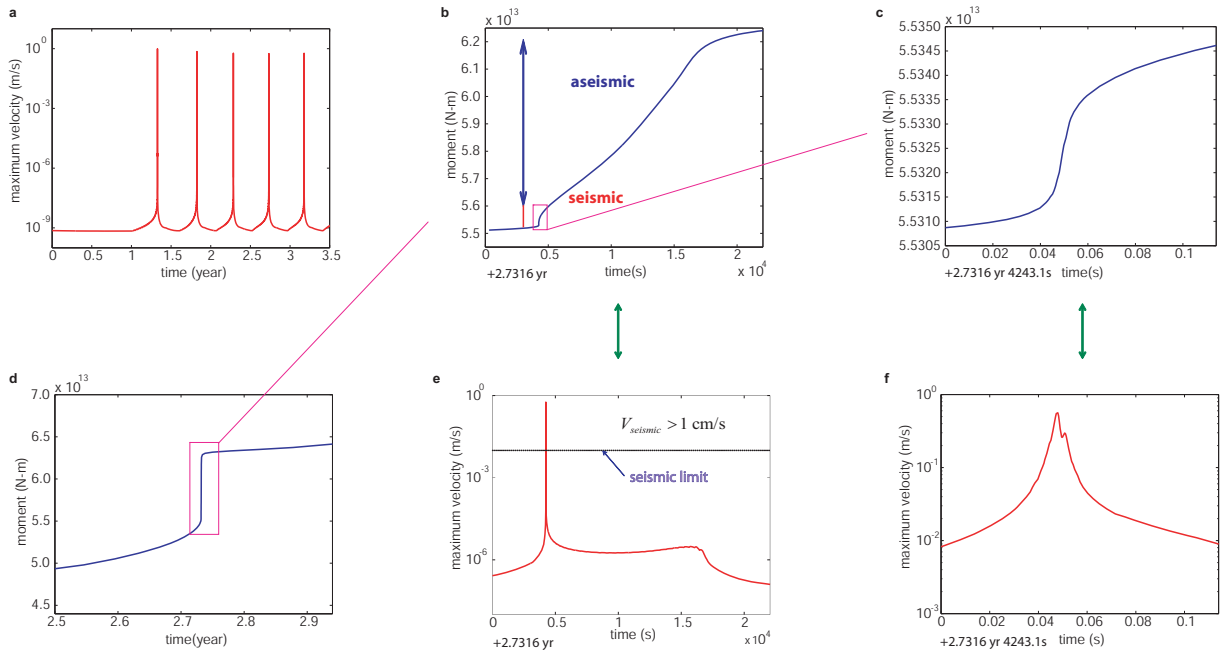

Figure 2. A simulation example that results in repeating earthquakes. We use the following parameters in this simulation: $V_{pl} = 23$ mm/yr, $L = 160$ microns, $f_o = 0.6$, $V_o = 10^{-6}$ m/s; patch radius $r = 124$ m, $a = 0.014$ and $b = 0.019$ in the patch, $a = 0.019$ and $b = 0.014$ in the velocity-strengthening zone. Column 1, top panel: Maximum slip velocity on the fault (on the logarithmic scale) is plotted as a function of time in years. Vertical lines correspond to dynamic events. After an initial phase determined by initial conditions, the model produces periodic repeating earthquakes. Slip velocity during dynamic events reaches values close to 1 m/s. In the interseismic period, maximum slip velocity is close to the loading (plate) rate. Column 1, bottom panel: The moment released on the velocity-weakening patch around the time of one of the repeating earthquakes. This is the fourth event simulated in the model. On this scale of years, the moment release looks abrupt. However, as we zoom in and plot moment release on the scale of 10,000 seconds (column 2, top panel), we see that what looked like seismic moment release actually occurs over the time of 10,000 seconds or so. The bottom panel in column 2 plots maximum slip velocity over the fault in the same time period and confirms that, during much of the moment release, slip velocity is close to 10^{-6} m/s which is 1 micron/s, definitely not a seismic value. Column 3 shows the corresponding plots for the time scale of order 0.1 seconds; note the significant change in scale for the moment in top panel and slip velocity in the bottom panel. The bottom panel of column 1 indicates that about 10^{13} N-m of moment is released close to the time of the repeating earthquake, while the top panel of column 3 indicates that only about 2 x 10^{11} N-m of that moment is released seismically. This makes the seismic moment released on the velocity-weakening patch about 50 times smaller than the aseismic moment.

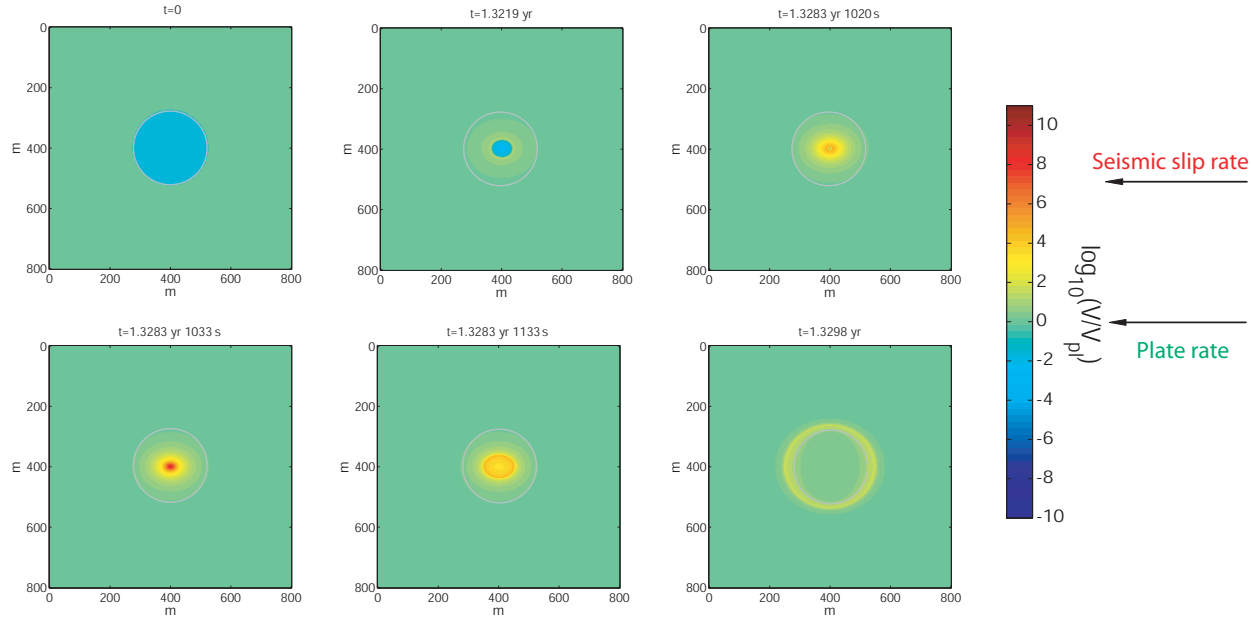

Figure 3. Snapshots of the slip velocity distribution over the simulated fault segment (800 m x 800 m) for the first event of the simulation example of Figure 2. Slip velocity is color-coded on the logarithmic scale. The seismic range of slip velocities (or rates) is indicated by red colors, slip velocities close to the loading rate are indicated by green colors, and creep with slip velocities faster than the plate rate is indicated by transitional yellow and orange colors. The location of the patch is outlined by a circle. The snapshot time is given above each panel. Row 1, left panel: At the beginning of the simulation, the patch is locked (with rates much lower than the loading rate) and the surrounding creeping zone is close to the loading rate. Row 1, middle panel: In 1.3219 years, the locked region shrinks to the area much smaller than the patch, with the edges of the locked region creeping because of stress concentrations there. Row 1, right panel: This snapshot is about two days later and shows that the previously locked patch experiences aseismic slip. That can be called the nucleation process, as 13 seconds later slip velocities reach seismic values (row 2, left panel). Note that the extent of high slip velocities is much smaller than the size of the patch. Row 2, middle panel: This snapshot is 100 seconds after the seismic event and shows postseismic creep over a significant part of the patch. The postseismic creep migrates outwards, as the next snapshot, taken several hours later, shows (row 2, left panel).

the edges of the velocity-weakening patch experience stress concentrations due to aseismic creep in the surrponding zone, and hence creep a lot themselves, leaving no room for seismic slip to occur there. This means that the sizes of repeating earthquakes inferred based on seismic data may be much smaller than the underlying velocity-weakening patches that cause them.

We can also estimate the (static) stress drop for repeating earthquakes by subtracting shear stress after an event from shear stress before the event. Stress drop over a cross-section centered on the patch, and along the *x*-direction, is shown in Figure 4b. Note that stress drop is concentrated in a small area compared to the size of the patch, consistently with the extent of seismic slip. The peak stress drop is of the order of 10 MPa, and the average stress drop over the area of stress change is of the order of 1 MPa for the events we simulated. Hence the values of

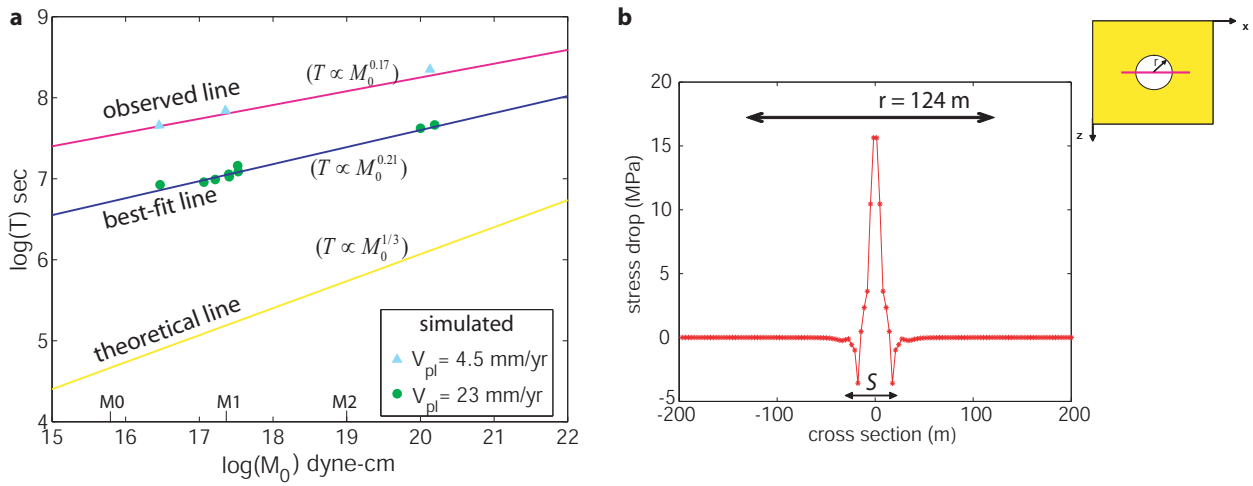

Figure 4. Left panel: Scaling of the repeat (or recurrence) time T with the seismic moment M_0. The top line indicates the best fit to observations of repeating earthquakes at Parkfield as given by Nadeau and Johnson (1998). The middle (blue) line shows the best fit to results of our simulations, which are indicated by green dots. These simulations are done with the same parameters as given in the caption to Figure 2, in particular, with the loading rate of $V_{pl} = 23$ mm/yr. Different seismic moments of repeating earthquakes are obtained by varying the radius of the velocity-weakening patch. Note that the slope of the scaling is matched very well, but the repeat times are shorter in our simulations than in the observations. If we use the applied loading rate of 4.5 mm/yr, which is within the range of 4 to 35 mm/yr suggested by Harris and Segall (1987) for the portion of the San Andreas fault with repeating earthquakes, then our model can reproduce both the scaling and the absolute values of the observed repeat times, as shown by blue triangles which are located around the line fit to observations (top line). Note that repeat times can also be changed in our models by changing friction properties, and this is one of the findings of our study. The bottom (yellow) line shows the theoretical scaling that matches regular earthquakes. That scaling has a wrong slope and severely underestimates the repeat times.

Right panel: Static stress drop along the line passing through the middle of the velocity-weakening patch as indicated on the insert. The stress drop is computed by subtracting shear stress at each spatial cell before and after the earthquake. We see that a significant stress change occurs only within the patch of 10-20 meters, while the diameter of the patch is 2 x 124 = 248 meters. The stress drop is variable in space, with the edges of the sliding zone showing a negative stress drop, which means that shear stress is actually increased there. This increased shear stress causes significant postseismic slip which, in turn, creates stress concentration in front of itself and hence migrates to the edges of the patch and into the velocity-strengthening zone. Note that the average stress drop over the region of stress change is in the range of 1-10 MPa, which is the typically observed range.

stress drops our model predicts are within the range of typical seismic estimates (e.g., Abercrombie, 1995). Such typical stress drops are also consistent with seismic inversions of repeating earthquakes based on seismic data from SAFOD (Imanishi et al., 2004).

References

Ampuero, J.-P., and A. M. Rubin, Earthquake nucleation on rate and state faults - Aging and slip laws, submitted to *J. Geophys. Res*., 2007.

Bayart, E., A. M. Rubin, and C. Marone, Evolution of Fault Friction Following Large Velocity Jumps, *Eos Trans. AGU*, **87**(52), Fall Meet. Suppl., S31A-0180, 2006.

Beeler, N. M., D. L. Lockner, and S. H. Hickman, A simple stick-slip and creep-slip model for repeating earthquakes and its implication for microearthquakes at Parkfield, *Bull. Seismol. Soc. Am*., **91**, 1797– 1804, 2001.

Ben-Zion, Y. and J. R. Rice, Dynamic simulations of slip on a smooth fault in an elastic solid, *J. Geophys. Res.*, **102**, 17771-17784, 1997.

Blanpied, M. L., D. A. Lockner and J. D. Byerlee, Fault stability inferred from granite sliding experiments at hydrothermal conditions, *Geophys. Res. Letters*, **18** (4), 609-612, 1991.

Blanpied, M. L., D. A. Lockner and J. D. Byerlee, Frictional slip of granite at hydrothermal conditions, *J. Geophys. Res*., **100**, 13045-13064, 1995.

Chen, T. and N. Lapusta, Scaling of seismic moment with recurrence interval for small repeating earthquakes simulated on rate-and-state faults, *Eos Trans. AGU*, 87(52), Fall Meet. Suppl., S23C-0187, 2006.

Chen, T. and N. Lapusta, Scaling of small repeating earthquakes explained by interaction of seismic and aseismic slip in a rate and state fault model, submitted to *J. Geophys. Res.*, 2008.

Chen, H. and R. Rau, Fault slip rates from repeating microearthquakes on the Chihshang fault, eastern Taiwan, *EOS Trans. AGU*, 84(46), Fall Meet. Suppl., Abstract T11F-06, 2003.

Cochard, A. and R. Madariaga, Complexity of seismicity due to highly rate dependent friction, *J. Geophys. Res*., **101** (B11), 25321-25336, 1996.

Day, S. M., L. A. Dalguer, N. Lapusta, and Y. Liu, Comparison of finite difference and boundary integral solutions to spontaneous rupture, *J. Geophys. Res.* 108, doi: 10.1029/2001JB000793, 2005.

Dieterich, J. H., Modeling of rock friction- 1 Experimental results and constitutive equations, *J. Geophys. Res.*, **84**, 2161-2168, 1979.

Dieterich, J. H., Constitutive properties of faults with simulated gouge, in *Mech. Beh. Crustal Rocks*, Geophys. Monogr. Ser., **24**, ed. by N. L. Carter, M. Friedman, J. M. Logan and D. W. Stearns, AGU, Washington, DC, 103-120, 1981.

Ellsworth, W.L. and G.C. Beroza, Seismic evidence for an earthquake nucleation phase, *Science*, **268**, 851-855, 1995.

Ellsworth, W. L. and L. D. Dietz, Repeating earthquakes: characteristics and implications, Proc. of Workshop 46, the 7th U.S.-Japan Seminar on Earthquake prediction, U.S.Geol.Surv. Open-File Rept. 90-98, 226-245, 1990.

Geubelle, P. and J. R. Rice, A spectral method for 3D elastodynamic fracture problems, *J. Mech. Phys. Solids*, **43**, 1791-1824, 1995.

Gu, J. C., J. R. Rice, A. L. Ruina, and S. T. Tse, Slip motion and stability of a single degree of freedom elastic system with rate and state dependent friction, *J. Mech. Phys. Solids*, 32, 167-196, 1984.

Harris, R. A., and P. Segall, Detection of a locked zone at depth on the Parkfield, California, segment of the San-Andreas fault, *J. Geophys. Res.* 92, B8, 7945-7962, 1987.

Ide, S., and M. Takeo, Determination of constitutive relations of fault slip based on seismic wave analysis, *J. Geophys. Res.*, **102**, 27,379– 27,391, 1997.

Igarashi, T., Matsuzawa, T., and A. Hasegawa, Repeating earthquakes and interplate aseismic slip in the northeastern Japan subduction zone, *J. Geophys. Res.* 108, B5, 2249, 2003.

Imanishi, K., W. L. Ellsworth, S. G. Prejean, Earthquake source parameters determined by the SAFOD Pilot Hole seismic array, *Geophys. Res. Letters*, **31**, L12S09, doi:10.1029/2004GL019420, 2004.

Komatitsch, D., Liu, Q., Tromp, J., Süss, P., Stidham, C., and Shaw, J., Simulations of ground motion in the Los Angeles basin based upon the spectral-element method, *Bull. Seism. Soc. Amer*., **94**, No.1, 187-206, 2004.

Lapusta, N., and Y. Liu, Three-dimensional elastodynamic simulations of seismic and aseismic slip history of a planar strike-slip fault, *Eos Trans. AGU*, 87(52), Fall Meet. Suppl., S34A-07, 2006.

Lapusta, N, and Y. Liu (2008), 3D boundary-integral modeling of spontaneous earthquake sequences and aseismic slip, submitted to *J. Geophys. Res.*, 2008.

Lapusta, N., J. R. Rice, Y. Ben-Zion, and G. Zheng, Elastodynamic analysis for slow tectonic loading with spontaneous rupture episodes on faults with rate- and state-dependent friction, *J. Geophys. Res*. 105, 23765-23789, 2000.

Lapusta, N. and J. R. Rice, Earthquake sequences on rate and state faults with strong dynamic weakening, *Eos Trans. AGU*, 85(47), T22A-05, 2004.

Liu, Y., and N. Lapusta, Three-dimensional simulations of spontaneous earthquake sequences, *Eos Trans. AGU*, 86(52), S43A-1068, 2005, manuscript in preparation, 2007.

Marone, C., Vidale, J. E., and W. L. Ellsworth, Fault healing inferred from time-dependent variations in-source properties of repeating earthquakes, *Geophys. Res. Lett.*, 22, 3095-3098, 1995.

Nadeau, R. M., and L. R. Johnson, Seismological studies at Parkfield VI: Moment release rates and estimates of source parameters for small repeating earthquakes, *Bull. Seism. Soc. Am.*, 88, 3, 790-814, 1998.

Nadeau, R. M., A. Michelini, R. A. Uhrhammer, D. Dolenc, T. V. McEvilly, Detailed kinematics, structure and recurrence of micro-seismicity in the SAFOD target region, *Geophys. Res. Letters*, **31**, L12S08, doi:10.1029/2003GL019409, 2004.

Perrin, G., J. R. Rice, and G. Zheng, Self-healing slip pulse on a frictional surface, *J. Mech. Phys. Solids*, **43**, 1461-1495, 1995.

Rice, J. R., Spatio-temporal complexity of slip on a fault, *J. Geophys. Res*., **98**, 9885-9907, 1993.

Rice, J. R., Heating and weakening of faults during earthquake slip, *J. Geophys. Res*., doi:10.1029/2005JB004006, 2006.

Rice, J. R., and Y. Ben-Zion, Slip complexity in earthquake fault models, *Proc. Natl. Acad. Sci. USA*, **93**, 3811-3818, 1996.

Rice, J. R., N. Lapusta, and K. Ranjith, Rate and state dependent friction and the stability of sliding between elastically deformable solids, *J. Mech. Phys. Solids* 49, 1865-1898, 2001.

Rice, J. R., and A. L. Ruina, Stability of a steady frictional slipping, *J. Appl. Mech*., 50, 343-349, 1983.

Rubin, A.M., and J.-P. Ampuero, Earthquake nucleation on (aging) rate and state faults, *J. Geophys. Res.*, 110, doi:10.1029/2005JB003686, 2005.

Ruina, A. L., Slip instability and state variable friction laws, *J. Geophys. Res*., **88**, 10359-10370, 1983.

Sammis, C. G., and J. R. Rice, Repeating earthquakes as low-stress-drop events at a border between locked and creeping fault patches, *Bull. Seism. Soc. Am.*, 91, 3, 532-537, 2001.
Shaw, B. E., and J. R. Rice, Existence of continuum complexity in the elastodynamics of repeated fault ruptures, *J. Geophys. Res*. 105, 23,791-23,810, 2000.
Shibazaki, B. and M. Matsu'ura, Spontaneous processes for nucleation, dynamic propagation, and stop of earthquake rupture, *Geophys. Res. Lett*., **19**, 1189-1192, 1992.
Vidale, J. E., Ellsworth, W. L., Cole, A., and C. Marone, Variations in rupture process with recurrence interval in a repeated small earthquake, *Nature*, 368, 6472, 624-626, 1994.